Eur. Phys. J. A **27**, s01, 83–88 (2006)
DOI: 10.1140/epja/i2006-08-012-y

EPJ A direct
electronic only

Experimental and theoretical screening energies for the ^{2}H(d, p)^{3}H reaction in metallic environments

K. Czerski[1,2,a], A. Huke[1], P. Heide[1], and G. Ruprecht[1,3]

[1] Institut für Atomare Physik und Fachdidaktik, Technische Universität Berlin, Hardenbergstr. 36, 10623 Berlin, Germany
[2] Institute of Physics, University of Szczecin, Szczecin, Poland
[3] TRIUMF, Vancouver, Canada

Received: 13 July 2005 /
Published online: 23 February 2006 –

Abstract. The study of the ^{2}H(d, p)^{3}H reaction at very low energies in deuterized metallic targets provides a unique possibility to test models of the electron screening developed for dense astrophysical plasmas. Here, we compare the experimental screening energies obtained by our group as well as by other authors for different target materials with theoretical predictions based on an improved dielectric function theory. The calculations are performed within the self-consistent regime and include polarization of both quasi-free and bound electrons. Additionally, the cohesion screening, arising from different binding energies of deuterons and α-particles in crystal lattices, is taken into account. The proposed theory predicts only a weak material dependence of the screening energy in agreement with our experimental results but fails in the absolute strength of the effect by a factor of 2. The projectile-velocity dependence of the screening energy corresponding to the transition from the weak-screening regime to the strong-screening limit is discussed.

PACS. 25.45.Hi Transfer reactions – 95.30.Dr Atomic processes and interactions – 95.30.-k Fundamental aspects of astrophysics

1 Introduction

Electron screening of the Coulomb barrier between reacting nuclei leads to an enhancement of thermonuclear rates in dense astrophysical plasmas. For so-called weakly coupled plasmas (for example our Sun), where the kinetic energy of plasma particles is larger than the mean Coulomb repulsion energy, the electron screening contributes only to a few percent and can be described within the Debye-Hückel model [1] of the nearly perfect stellar gas. In the opposite limit of strongly coupled plasmas, at high densities and low temperatures the electron gas is degenerate and the ions undergo long-range correlation forces forming either a quantum liquid or a Coulomb lattice beyond a critical density. In such a case nuclear reaction rates can be increased by many orders of magnitude and are probably realized in White and Brown Dwarfs or Giant Planets. The study of d + d nuclear reactions at very low energies on deuterons embedded in metallic lattices makes it possible to test models of the electron screening developed for dense astrophysical plasmas in the terrestrial laboratory. The exponential-like increase of the reaction cross-section observed for decreasing projectile energies, as compared to the cross-section for bare nuclei, can be described by a screening energy. As could be shown in our first experiments [2,3], the screening energies determined for the d + d fusion reactions in metallic environments are by about a factor of 10 larger than that observed for the gas target [4] and up to a factor of 4 larger than the theoretical predictions [5]. This finding was also confirmed by results of other groups [6,7,8,9,10,11]. Especially, the data obtained by the LUNA Collaboration for almost 60 different target materials [11] enable us to compare the experimental results of different groups and to look for a theoretical description of the observed target material dependence as well as of the absolute screening energy values. The approach presented here is based on an improved dielectric function theory [12,13] that allows to derive a reliable deuteron-deuteron potential in the host metal including contributions not only from quasi-free valence electrons but also from polarized bound electrons. A special interest will be devoted to the dependence of the screening energy on projectile energies.

2 Experimental screening energy

Our experiments have been performed [3,13,14] using the D^+ and D_2^+ beams accelerated to energies between 5 and

[a] e-mail: czerski@kalium.physik.tu-berlin.de

60 keV and impinged on metallic targets (Li, Al, Zr, Pd and Ta) and amorphous graphite carbon foils. Most of the targets were implanted to large deuteron densities corresponding approximately to the chemically stable stoichiometry. In the case of Pd the implantation process was interrupted at a relatively small deuteron density (stoichiometric ratio $n_{\mathrm{d}}/n_{\mathrm{Pd}} \approx 0.3$) in order to study fusion reactions in the metallic environment possessing a small number of crystal-lattice defects and reducing the number of possible deuterium bubbles resulting from long-term irradiation. The deuteron density used for the Li target was even smaller ($n_{\mathrm{d}}/n_{\mathrm{Li}} \approx 0.03$) to prevent the target from oxidation. The reaction products (protons, tritons and ^{3}He particles) were detected by four Si detectors located in the reaction plane at backward angles.

The experimental determination of the electron screening energy is based on the assumption that the observed exponential-like enhancement of the reaction yield towards low projectile energies results from the reduction of the height of the Coulomb barrier. In the simple case of Bohr screening, the screened Coulomb potential energy between two reacting deuterons can be presented as follows:

$$V(r) = \frac{e^2}{r} \exp\left(-\frac{r}{a}\right) \approx \frac{e^2}{r} - \frac{e^2}{a}, \tag{1}$$

where a is the screening length being of the order of the Bohr radius. For projectile energies used in accelerator experiments where $r \ll a$, the deuteron-deuteron potential can be simply described as the Coulomb potential reduced by a constant, the screening energy $U_e = e^2/a$. Thus, the "screened" cross-section, applying the transformation to the only weakly on energy dependent astrophysical S-factor, reads as follows:

$$\sigma_{scr}(E_{cm}) = \frac{1}{\sqrt{E_{cm}(E_{cm}+U_e)}} S(E_{cm}) \times \exp\left(-\sqrt{\frac{E_G}{E_{cm}+U_e}}\right). \tag{2}$$

Here E_{cm} denotes the energy in the center-of-mass system and E_G is the Gamow energy. The screening energy U_e takes into account a drop of the Coulomb barrier in the expression for the penetration factor. In the experiment the strength of the screening effect is described by means of the thick-target enhancement factor $F(E)$ defined as the ratio between the angular integrated thick-target yields for screened and bare nuclei [3],

$$F(E) = \frac{Y_{scr}(E)}{Y_{bare}(E)} = \frac{\int_0^E \frac{\sigma_{scr}(E)}{\varepsilon(E)}\,\mathrm{d}E}{\int_0^E \frac{\sigma(E)}{\varepsilon(E)}\,\mathrm{d}E} = \frac{\int_0^E \frac{\sigma_{scr}(E)}{\sqrt{E}}\,\mathrm{d}E}{\int_0^E \frac{\sigma(E)}{\sqrt{E}}\,\mathrm{d}E}. \tag{3}$$

Here, $\sigma(E)$ and $\varepsilon(E)$ are the cross-sections for bare nuclei and the stopping power taken at the beam energy E, respectively. The enhancement factor $F(E)$ is independent of the target deuteron density and of the absolute value of the stopping power; the only assumption used is that $\varepsilon(E) \propto E^{1/2}$ which agrees with the experimental data for all target materials investigated. The bare-nuclei cross-section is very well known from the precision measurements performed with the gas target [15]. From the exponential increase of $F(E)$ towards lower projectile energies the screening energy U_e can be determined. The U_e values obtained in our experiments for C, Li, Al, Zr, Pd and Ta targets are presented in fig. 2. For heavier metals the screening energy amounts to about 300 eV which is one order of magnitude larger than the value 25 ± 5 eV obtained in the gas target experiment [4].

3 Theoretical description of the electron screening effect

A charge point impurity embedded in a metallic environment leads to a polarization of surrounding degenerate electrons causing a cut-off of the screened Coulomb field at a characteristic distance of the inverse of the Fermi wave number. Additionally, the bound electrons of the host metal can also be polarized and contribute to the screening. Thus, using the standard Fourier representation of $1/r$, the screened Coulomb potential energy $V(r)$ between reacting deuterons within a static approximation can be expressed as follows [13]:

$$V(r) = \frac{e^2}{r}\Phi(r) = \frac{1}{(2\pi)^3}\int \frac{4\pi\left(e\varphi(q)\right)^2}{\varepsilon_\nu(q)\,\varepsilon_c(q)\,q^2}\exp(i\boldsymbol{qr})\,\mathrm{d}^3q, \tag{4}$$

where $\varepsilon_\nu(q)$ and $\varepsilon_c(q)$ are the static wave-number–dependent dielectric functions resulting from quasi-free valence electrons and from bound metallic core electrons, respectively, and $\Phi(r)$ denotes the screening function. The elementary charge e is multiplied by a self-consistent charge form factor $\varphi(q)$ for deuterons with the screening electrons in the Thomas-Fermi approximation:

$$\varphi(q) = 1 - z + zq^2/\left(q^2 + k_{TF}^2\right). \tag{5}$$

Here, the Thomas-Fermi wave number $k_{TF}^2 = 6\pi e^2 n/E_F$ has been used; n and E_F are the electron number density and the Fermi energy, respectively. The number z corresponds to the fraction of electrons bound to deuterons and can vary between 0 and 1. Since we are interested in the evaluation of the strongest possible screening effect, we set $z = 1$. In the absence of screening $\varepsilon_\nu \equiv \varepsilon_c \equiv 1$ and $z = 0$, $V(r)$ reduces to the bare Coulomb potential ($\Phi(r) \equiv 1$). The response of the valence electron gas to an external field is given by the dielectric function:

$$\varepsilon_\nu(q) = 1 - \frac{\nu(q)\,P(q)}{1 + \nu(q)\,G(q)\,P(q)}, \tag{6}$$

where $\nu(q) = 4\pi e^2/q^2$ and $P(q)$ is the static Lindhard RPA polarizability [16]. $G(q)$ is the static local field correction that takes into account the short-range electron correlation and the exchange interaction [17].

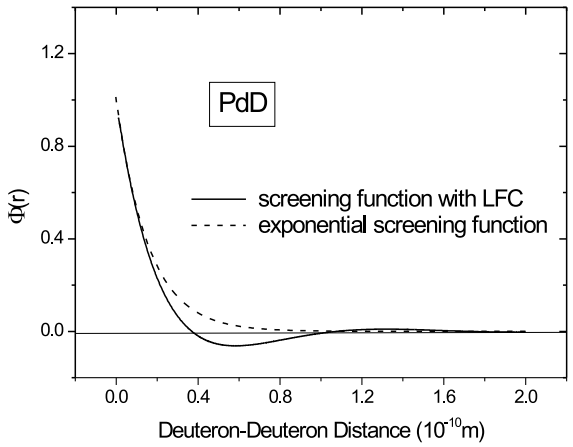

Fig. 1. Screening function calculated for PdD with the local field correction (LFC). For comparison the Bohr screening function with the same screening length is presented.

If we set $G(q) = 1$ and apply the long-wave approximation [12], the expression for the valence electron dielectric function (eq. (6)) reduces to the Thomas-Fermi form

$$\varepsilon_{TF}(q) = 1 + \frac{k_{TF}^2}{q^2}\,. \tag{7}$$

In this case the screening function can be described by the exponential function $\exp(-k_{TF}r)$ leading to the screening energy $e^2 k_{TF} = e^2(4me^2/\pi\hbar^2)^{1/2}(3\pi 2n)^{1/6}$. Hence, the corresponding value depends only weakly on the electron density and amounts for Pd to 54 eV.

In the case of core electron polarization we applied the dielectric function proposed in [18]. Different from the valence electron polarization, ε_c takes a finite value at the limit $q = 0$. In the case of Ta the core-dielectric constant $\varepsilon_c(0) = 3.21$. The screening function $\Phi(r)$ calculated by a numeric integration of eq. (4) differs from the simple Bohr screening $\exp(-r/a)$ particularly for larger distances where the numeric potential becomes negative and shows characteristic Friedel oscillations. For smaller distances the potential becomes attractive reducing appropriately the screening length (see fig. 1).

In the metallic lattice, besides electrons also positive ions can contribute to the screening of the Coulomb barrier between reacting nuclei. This effect, called cohesion screening, can be calculated in analogy to the dense astrophysical plasmas within the ion-sphere model of Salpeter [1] providing in the case of the TaD target a screening energy of 18 eV. In our calculations we used a more realistic model based on the universal ion-ion potential introduced by Biersack [19]. This potential describes the interaction between light ions as well as between heavy ions at low energies with very good accuracy. Since the potential energy of two deuterons in the field of a host metal atom is larger than that of the helium atom produced in the fusion reaction, one obtains a gain in potential energy. For a rough estimation of the cohesion screening energy U_{coh}, we calculated the potential energy gain resulting from the surrounding 12 host atoms assuming the same fcc crystal structure for all target materials investigated [13].

The above description of the screening effect is limited to the charged particles with a velocity lower than the Fermi velocity v_F, for which the adiabatic approximation can be used. For higher velocities the electrons have not enough time to follow the ions and a wake wave [20] trails the ion through the electron gas. Thus, the electron screening gets weaker and depends on the velocity v of the ion. The screening length for the dynamic screening can be expressed by $a_d = v/\omega_p$, where ω_p is the plasmon frequency $\omega_p^2 = 4\pi ne^2/m$. Since the ion velocity v can be treated as velocity of electrons relative to the resting ion, the dynamic screening can also be applied to hot plasmas where the electron velocity arises from the plasma temperature T. Then $v^2 = k_B T/m$, where k_B is the Boltzmann constant. Consequently, the screening length in a hot plasma reads as follows:

$$a_{hp}^2 = \frac{k_B T}{4\pi e^2 n} \tag{8}$$

which corresponds to the Debye radius determining the electron screening within the Debye-Hückel model. In this sense, the velocity dependence of the screening length can describe the transition between a weak electron screening (hot plasmas) for $v > v_F$ and the strong electron screening (cold plasmas) for $v < v_F$. A corresponding formula has been proposed by Lifschitz and Arista [21],

$$\frac{1}{a^2(v)} = \gamma\frac{2v_F}{\pi}\left(1 + \frac{v_F^2 - v^2}{2v_F v}\ln\left|\frac{v + v_F}{v - v_F}\right|\right), \tag{9}$$

where γ is a number factor depending on the form of the screening function $\Phi(r)$. For small v the expression in parenthesis reaches the limit of 2 and the screening length its minimum value (strong screening).

Since the deuteron energies, for which an enhancement of the d + d reaction cross-sections due to the electron screening can be observed, are smaller than the corresponding deuteron Fermi energy (for Al $E_F(\mathrm{d}) = 46$ keV),

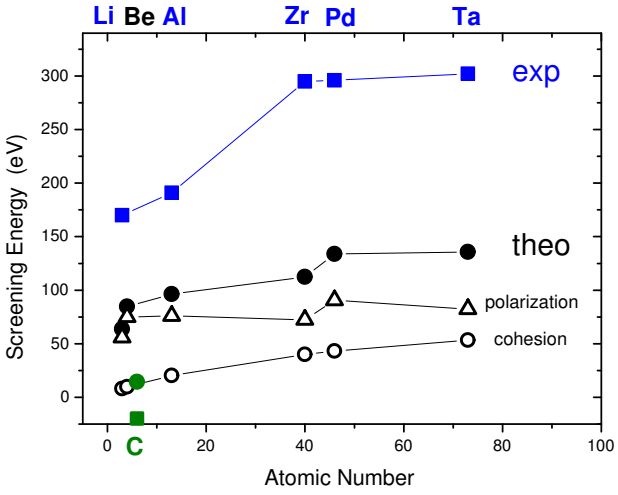

Fig. 2. Experimental and theoretical electron screening energies.

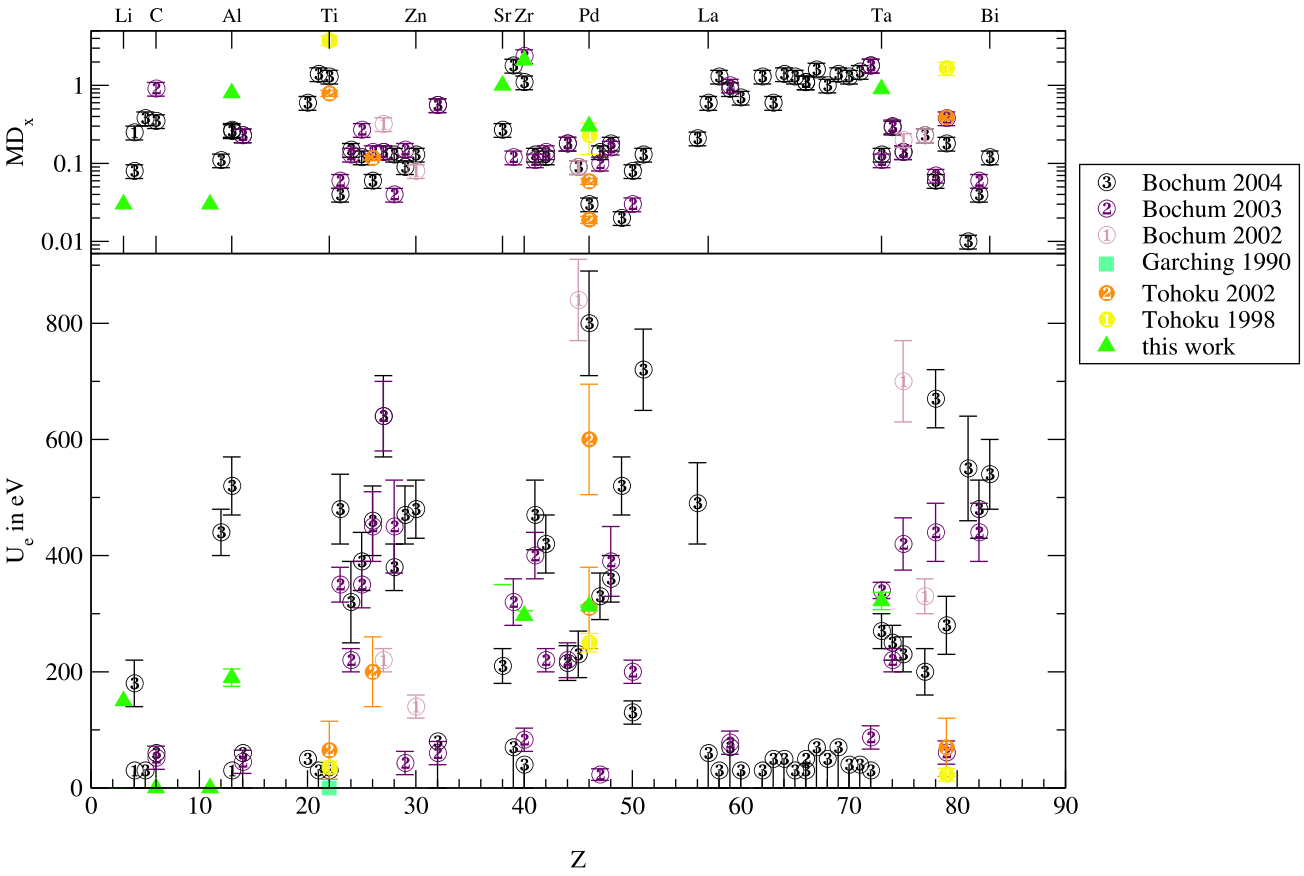

Fig. 3. Comparison of experimental screening energies. Also depicted are the corresponding densities of the implanted deuterons.

we consider the experimentally determined screening energy independent of velocity. Thus, the experimental values of U_e can be directly compared with the theoretical ones according to the prescription

$$U_{pol} = \lim_{r \to 0} \left(\frac{e^2}{r} - \frac{e^2}{r} \Phi(r) \right). \quad (10)$$

The theoretical value for the total electron screening energy U_e is a sum of the polarization and cohesion screening energies $U_{pol} + U_{coh}$. The theoretical and experimental U_e values determined for all target materials we have investigated are presented in fig. 2.

The theoretical calculations describe the observed material dependence of the screening energy qualitatively correctly. The main contribution to the theoretical values is provided by polarization of the free valence electrons [13], although the contribution of bound electrons (core polarization) cannot be neglected. In the case of TaD, the resulting core polarization energy amounts to about 1/3 of the valence electron screening energy. An increase of U_e with the atomic number arises mainly from the cohesion contribution. However, the absolute values of the theoretically calculated U_e fail by a factor of about two as compared to our experimental values. Including the self-consistent correction and the full wave number dependence of the dielectric function leads to screening energies lower than those determined within the simplified theory [12]. No reason for such a large discrepancy between theoretical and experimental values has been found so far. Even if a possible contribution of the channeling effect to the experimentally determined U_e values would be taken into account —in the case of Ta much smaller than 100 eV [22]— the difference between experiment and theory remains large.

4 Comparison with results of other authors

The screening energies measured by different groups together with the deuteron densities achieved in the experiments are presented in fig. 3. The largest part of data was obtained by the LUNA Collaboration (Bochum group) which measured the screening energies for more than 50 metals in three different experiments. Compared to our U_e values that show only a weak material dependence and a kind of saturation for heavier metals (Zr, Pd, Ta) with a screening energy of about 300 eV, there are partially large deviations.

The screening energy determined for Ta by the LUNA Collaboration [8] (309 ± 12 eV) and for Pd by the Japanese group (Tohoku 1998 and 2002) [6,7] (310 ± 50 eV) are very close to our values 302 ± 13 eV and 296 ± 15 eV, respectively. On the other hand, the corresponding Pd

value obtained by the LUNA Collaboration is much larger amounting to 800 ± 90 eV [11]. For Zr the LUNA Collaboration reported a significantly smaller U_e value than ours, whereas the values obtained for Al changed from a low value in the first experiment to a large one in the third experiment where the target surface was cleaned by Kr sputtering immediately before the deuteron incidence.

The strong variation of the experimental screening energies for different metals, as depicted in fig. 3, contradicts our results and cannot be explained within the proposed theory. For some metals, the experimental screening energies are even smaller than theoretical ones. In order to explain this, an application of the Debye-Hückel model was suggested [10,11,23]. The authors, setting room temperature into the expression for the Debye screening length (eq. (8)) and comparing with experimental U_e values, obtain charge carrier densities which are close to those determined from experimental Hall constants. Consequently, the experimental screening energies should be dependent on temperature and proportional to the density of charge carriers, *i.e.* electrons and holes. However, as shown in the previous section, the Debye-Hückel screening is applicable only for large temperature ($k_BT > E_F$) for which the electron degeneration vanishes and the Maxwell-Boltzmann statistics can be used. For low temperatures ($k_BT < E_F$) or correspondingly low projectile energies, the strong-screening limit should be applied. According to eq. (9), the screening length within this limit is smaller than the Debye length at the temperature $k_BT = E_F$ by a factor of $\sqrt{2}$. By the same factor the screening energy increases for low velocities. Additionally, no temperature dependence should be observed for the strong screening. Furthermore, the dominant contribution to the screening effect, the valence electron polarization, should only weakly depend on the electron density, in accordance with the Fermi-Dirac model $U_{FD} \propto n^{1/6}$ (see fig. 2).

Thus, the strong variation of U_e observed in some experiments probably arises from experimental problems with keeping constant a homogeneous deuteron density in the metallic targets. Contrary to our experiments, the large screening energies were measured using targets with relatively low deuteron densities. This can cause a temporal increase of the deuteron density in the surface region during the irradiation by projectile with lower energies and lead to an artificially large U_e values. In turn, too low screening energies can result from an oxidation layer on the target surface. Since the deuteron density in such a layer is much smaller than in the metallic bulk, the increase of the cross-section at low beam energy should be reduced [24]. Even cleaning of the target surface by a sputtering gun cannot help much under high-vacuum conditions, since in a vacuum of order 10^{-8} mbar the targets can re-oxidize within a few minutes (see, for example, [25]). This effect depends very strongly on the chemical reactivity of the target material and can be, on the other hand, reduced by the sputtering process of the target surface during the deuteron irradiation, which is, however, also target material dependent. Thus, the small value of U_e for some metals being significantly smaller than both our experimental and theoretical values, might be due to the re-oxidation process of the target. For a further detailed discussion of experimental results, we refer to our forthcoming paper [26].

5 Discussion and conclusions

In contradiction to results of the LUNA Collaboration, our experimental screening energies show only a weak target material dependence. As already stated above, discrepancies probably arise from an inhomogeneous depth distribution of deuterons within the irradiated targets. The situation can certainly be improved in the future experiments performed under ultra-high–vacuum conditions with an on-line monitoring of the deuteron density.

Clearly, the target material dependence of the screening energy is very important for the theoretical description of the effect. The improved dielectric function theory presented here supports a weak target material dependence of the screening energy. The theory provides, however, absolute values being by a factor of 2 smaller than the experimental ones. Therefore, one of the aims of future experiments remains to prove which screening contribution —valence electron polarization, core electron polarization or cohesion screening— is enhanced in the deuterized metals. Such a test is also very interesting for the physics of dense astrophysical plasmas. A large advantage of the presented theoretical approach is its ability to determine the deuteron-deuteron potential also for large distances (fig. 1). This enables to calculate the effective screening energies down to room temperature and consequently to compare the experimental results at higher energies with those achieved in the cold-fusion experiments by means of the heavy-water electrolysis. As shown in [13], the screening energy of order 300 eV determined in accelerator experiments can explain the neutron production rate observed by Jones *et al.* [27] at room temperature. Much larger U_e values of order 750 eV obtained in some accelerator experiments would increase the neutron production rate at room temperature by a factor of 10^7, which is, however, not observed.

The method proposed to include the velocity dependence for the dynamic screening allows to demonstrate the transition from the weak- to the strong-screening regime. Since the electron screening effect in the nuclear reactions is observable only at very low projectile energies, the theoretical description in the frame of the adiabatic dielectric function theory is well founded. On the contrary, the model based on the Debye-Hückel theory is for low temperatures and projectile velocities below the Fermi velocity not applicable.

References

1. E.E. Salpeter, Aust. J. Phys. **7**, 373 (1954).
2. K. Czerski, A. Huke, P. Heide, M. Hoeft, G. Ruprecht, in *Nuclei in the Cosmos V, Proceedings of the International Symposium on Nuclear Astrophysics, Volos, Greece, July 6-11 1998*, edited by N. Prantzos, S. Harissopulos (Editions Frontières, 1998) p. 152.

3. K. Czerski, A. Huke, A. Biller, P. Heide, M. Hoeft, G. Ruprecht, Europhys. Lett. **54**, 449 (2001).
4. U. Greife, F. Gorris, M. Junker, C. Rolfs, D. Zahnow, Z. Phys. A **351**, 107 (1995).
5. S. Ichimaru, Rev. Mod. Phys. **65**, 252 (1993).
6. H. Yuki, J. Kasagi, A.G. Lipson, T. Ohtsuki, T. Baba, T. Noda, B.F. Lyakhov, N. Asami, JETP Lett. **68**, 823 (1998).
7. J. Kasagi, H. Yuki, T. Baba, T. Noda, T. Ohtsuki, A.G. Lipson, J. Phys. Soc. Jpn. **71**, 2281 (2002).
8. F. Raiola *et al.*, Eur. Phys. J. A **13**, 377 (2002).
9. F. Raiola *et al.*, Phys. Lett. B **547**, 193 (2002).
10. C. Bonomo *et al.*, Nucl. Phys. A **719**, 37c (2003).
11. F. Raiola *et al.*, Eur. Phys. J. A **19**, 283 (2004).
12. K. Czerski, A. Huke, P. Heide, Nucl. Phys. A **719**, 52c (2003).
13. K. Czerski, A. Huke, P. Heide, G. Ruprecht, Europhys. Lett. **68**, 363 (2004).
14. A. Huke, *Die Deuteronen-Fusionsreaktionen in Metallen*, PhD Thesis, Technische Universität Berlin, (2002).
15. R.E. Brown, N. Jarmie, Phys. Rev. C **41**, 1391 (1990).
16. G. Grosso, G.P. Parravicini, *Solid State Physics* (Academic Press, 2000).
17. S. Moroni, D.M. Ceperley, G. Senatore, Phys. Rev. Lett. **75**, 689 (1995).
18. D.E. Penn, Phys. Rev. **128**, 2093 (1962).
19. J.F. Ziegler, J.P. Biersack, U. Littmark, *The Stopping and Ranges of Ions in Solids* (Pergamon Press, New York, 1985).
20. V.N. Neelevathi, R.H. Ritchie, W. Brandt, Phys. Rev. Lett. **302**, 302 (1974).
21. A.F. Lifschitz, N.R. Arista, Phys. Rev. A **57**, 200 (1998).
22. K. Czerski, A. Huke, P. Heide, G. Schiwietz, Nucl. Instrum. Methods B **193**, 183 (2002).
23. F. Raiola *et al.*, J. Phys. G **31**, 1141 (2005).
24. A. Huke, K. Czerski, P. Heide, Nucl. Phys. A **719**, 279c (2003).
25. K. Czerski *et al.*, Nucl. Instrum. Methods B **225**, 72 (2004).
26. A. Huke, K. Czerski, P. Heide, to be published.
27. S.E. Jones *et al.*, Nature **338**, 737 (1989).